Spectral-timing modelling of the X-ray reverberation in Mrk 335

Poemwai Chainakun & Andrew J. Young
H. H. Wills Physics Laboratory, Tyndall Avenue, Bristol, BS8 1TL, UK
Email: phxpc@bristol.ac.uk

University of BRISTOL

Introduction

We present a physical X-ray reverberation model (so called *REVB* model) to investigate the spectrum and time lags during the high flux state of Mrk 335 observed by *XMM-Newton* in 2006. The model consists of an isotropic-point source stationary on the symmetry axis of a black hole. A ray-tracing simulation is performed in parallel using GPUs to follow the photons between the source, the disc and an observer. We calculate the ionization state of each disc-annulus and employ *XILLVER* model (e.g., García+2013) to obtain the ionized back-scattered X-ray spectrum.

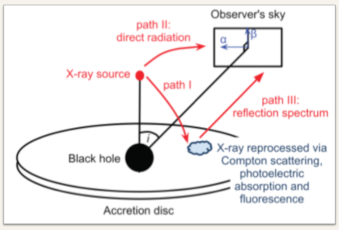

Figure 1: Sketch of the X-ray reverberation model (Chainakun & Young 2012).

Since the back-scattered photons take a longer time to reach the observer compared to the direct photons. The energy bands dominated by the reflection component will lag behind those bands dominated by the direct component. These lags referred to as reverberation lags are associated with the light-travel time between the source and the disc allowing us to probe the location and geometry of the X-ray source(s).

Modelling time-averaged and lag spectra

Frequency-dependent time lags are computed using the response functions taking into account full dilution effects (i.e. the suppression of lags because of contamination between cross-components in the soft- and hard-band light curves). The nature of reverberation lags has been investigated through a wide range of key parameters (e.g. Wilkins & Fabian 2013, Cackett+2014, Emmanoulopoulos +2014). Our model can simultaneously produce the time-averaged and lag spectra. Examples are shown in figure 2 for different values of the disc outer radius.

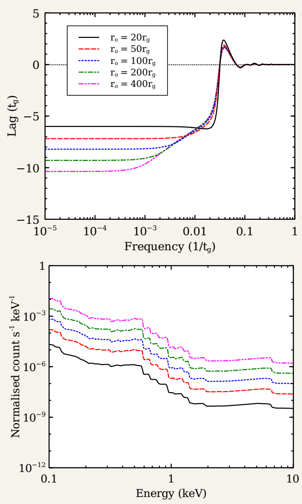

Figure 2: Frequency-dependent time lags (top) and the corresponding reflection spectra (bottom) for different values of the disc outer radius.

Effects of radial ionization gradients on time lags

The *REVB* can be used to investigate the cases of either constant or radially varying ionization parameter. The variations in flux-contamination can be physically produced when the ionization state of the disc changes in response to changes in the source luminosity. Even though the source height is fixed (the light-crossing distances are constant), the time lags decrease with increasing ionization state, and for the highly ionized disc the lags are very small (figure 3).

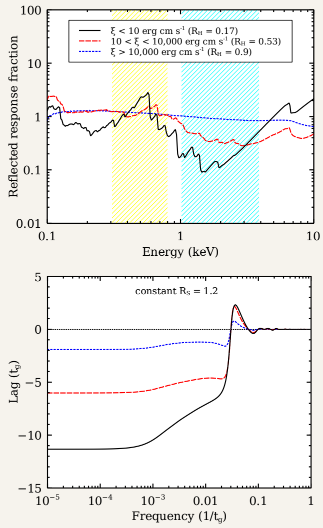

Figure 3: Reflected response fraction (top) in case of cold (black line), medium-ionized (red dashed line) and highly-ionized (blue dotted line) and their corresponding time lags (bottom).

Grid of *REVB* parameters and fitting procedure

To fit the data of Mrk 335, we produce the grid of *REVB* model as shown in table 1. The fitting procedure is performed in *ISIS.* The time lags were produced in a standard way, following the data reduction of Kara+2013.

Parameters	Value
source height (h/r_g)	2, 3, 4, 5, 6, 7, 8
inclination angle (i/degree)	15, 30, 45, 60
photon index (Γ)	1.8, 2, 2.2, 2.4
iron abundance (A)	0.5, 1, 2
log of ionization state ($\log \xi_{ms}$ / erg cm s^{-1})	1, 2, 3, 4, 5
disc density index (p)	0, 1, 2
soft reflected response fraction (R_S)	0.3, 0.4, 0.5, 0.6, 0.7, 0.8, 0.9, 1

Table 1: Grid of *REVB* parameters to fit Mrk 335. The spin parameter is fixed at 0.998 and the disc extends from r_{ms} to 400 r_g.

In *ISIS*, the *XMM-Newton* spectrum, background and responses are loaded as the first data set. We define a second data set which represents the time lag vs. frequency. The *REVB* model produces the time-averaged spectrum which is fit to the first data set and the time lag spectrum that is, simultaneously, fit to the second data set.

Spectral model requires 2 additional narrow Gaussians at ~6.4 and 7 keV interpreted as the distant reflection from molecular torus and the hot gas filling that torus, respectively.

Timing model requires additional power-law to produce the low-frequency positive lags that may be attributed to the propagation of fluctuations in the disc.

Results

We begin simultaneous fitting the 2-10 keV spectrum and time lags between 2.5-4 and 4-6.5 keV bands (figure 4). The best fitting parameters are listed in table 2.

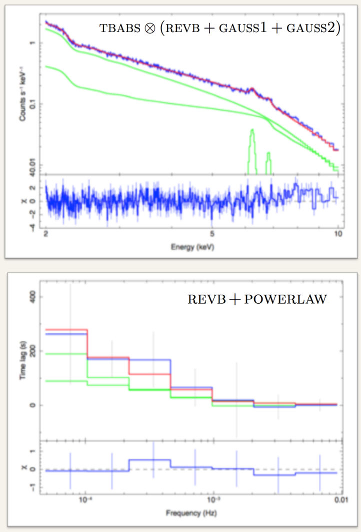

Figure 4: Data and residuals from simultaneously fitting the model to the spectra (top) and 2.5-4 vs. 4-6.5 keV lags (bottom).

Component	Parameter	Value
TBABS^s	$N_H (\times 10^{20}$ cm$^{-2})$	4.0^f
REVB^{s+t}	$h(r_g)$	2
	i (°)	45
	Γ	2.4
	A	0.5
	$\log \xi_{ms}$(erg cm s^{-1})	3
	p	0
	R_S	0.3
	Norm1	7.6×10^5
	$\log M (M_\odot)$	7.1
POWERLAW^t	s	0.82
	Norm2	151.8
GAUSS1^s	Area ($\times 10^{-6}$)	9.81^f
	Centre (keV)	6.4^f
GAUSS2^s	Area ($\times 10^{-6}$)	4.80^f
	Centre (keV)	7.0^f
χ^2/d.o.f.		1.026

Table 2: Model parameters for fits shown in figure 4. The superscript *s* refers to spectral parameters while *t* refers to timing parameters. The superscript *f* identifies the parameters which are fixed.

Finally, we fit the combined 0.3-10 keV spectrum and 0.3-0.8 vs. 1-4 keV lags (figure 5). We add a blackbody component and replace two Gaussians with unblurred-*XILLVER* and V*MEKAL* models. Most of the *REVB* parameters are comparable to what previously obtained.

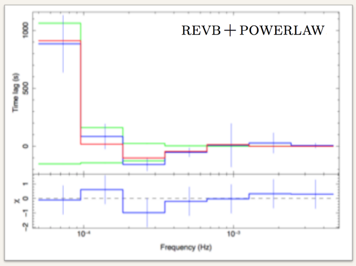

Figure 5: Data and residuals of 0.3-0.8 vs. 1-4 keV lags when simultaneous fitting with the 0.3-10 keV spectrum.

Conclusion

We successfully perform simultaneous fitting time-averaged spectrum and the soft- and hard-band lags of the high flux state of Mrk 335. The key parameters of this object (e.g. *h* and *M*) are constrained. The model is quite flexible and can be applied more broadly.

References: *Chainakun & Young 2015 (In Press), Chainakun & Young 2012, Wilkins & Fabian 2013, García+2013, Kara+2013, Cackett+2014, Emmanoulopoulos+2014*